

## LARGE AREA *n*-TYPE CZ DOUBLE SIDE CONTACTED BACK-JUNCTION BORON EMITTER SOLAR CELL

S. Bordihn<sup>1,2</sup>, V. Mertens<sup>1\*</sup>, P. Engelhart<sup>1</sup>, T. Florian<sup>1</sup>, J. Cieslak<sup>1</sup>, F. Stenzel<sup>1</sup>, P. Kappe<sup>1</sup>, T. Ballmann<sup>1</sup>,  
J.Y. Lee<sup>1</sup>, T. Lindner<sup>1</sup>, M. Junghänel<sup>1</sup>, J.W. Müller<sup>1</sup>, W.M.M. Kessels<sup>2</sup> and P. Wawer<sup>1</sup>

<sup>1</sup>Q-Cells SE, OT Thalheim, Sonnenallee 17-21, 06766 Bitterfeld-Wolfen

\*Phone: +49 (0)3494 66 99-52120; e-mail: [v.mertens@q-cells.com](mailto:v.mertens@q-cells.com)

<sup>2</sup>Department of Applied Physics, Eindhoven University of Technology, P.O. Box 513, 5600 Eindhoven, The Netherlands

**ABSTRACT:** The solar cell concept of a double side contacted back-junction high-efficiency *n*-type Si solar cell is presented. Numerical simulations were done with PC1D to evaluate the main loss mechanisms of the solar cell concept. The influence of bulk material properties and resistivity were investigated to find the requirements needed for large area *n*-type Si material. Analogous to simulations of Hermle *et al.* for back-junction back contact solar cells the sensitivity of the solar cell efficiency on the front side recombination was shown. The recombination of the metalized regions on the solar cell front captures a major role in efficiency limitation. Experimentally determined saturation current densities  $J_0$  on symmetrically processed lifetime test structures were used for an estimation of the open circuit voltage  $V_{oc}$  potential of the solar cell. The influence of solar cell rear side passivation layer on the limitation of efficiency was tested on the solar cell device level by comparing two different dielectric passivation layers. It is shown that an improvement of  $\Delta V_{oc} = 10$  mV was achieved with the optimized rear side passivation layer. Solar cell efficiencies of up to  $\eta = 20.2\%$  were realized and independently confirmed on a total area of 243.36 cm<sup>2</sup>.

**Keywords:** *n*-type back-junction solar cell, PC1D simulation, saturation current density

### 1 INTRODUCTION

For *n*-type Si solar cells the highest efficiencies for an industrial relevant process and related device area are reported by Cousins (Sunpower Corp.)  $\eta = 24.2\%$  [1] and by Sakata *et al.* (Sanyo)  $\eta = 23.1\%$  [2]. Despite the high level of efficiency provided by these solar cells other concepts are still under investigation. Solar efficiencies of  $\eta = 18.1\%$  (area 243 cm<sup>2</sup>) were achieved with the emitter-wrap through (EWT) concept using *n*-type Si. [3] Kiefer *et al.* reported  $\eta = 21.6\%$  solar efficiencies with the same concept on an area of 4 cm<sup>2</sup>. [3] The EWT solar cells provided both metal contacts present on the solar cell rear side. By following the approach of separating one metallization contact on the front and the other one on the rear side, as done for conventional industrial solar cells concepts such as the passivated emitter rear totally diffused (PERT) solar cells arise. Richter *et al.* presented on an area of 149 cm<sup>2</sup>  $\eta = 19.4\%$  and on 4 cm<sup>2</sup>  $\eta = 20.8\%$  solar cell efficiencies using this PERT solar cell concept. [4] The concept was done with the Aerosol jet printing technique for the front side metallization. Therefore a boron emitter on the front side requires a detailed understanding and new techniques for the contact formation. Glunz *et al.* addressed recently the challenges for realization of industrial large area *n*-type Si solar cells. [5] As reported by Engelhart an evolutionary way of solar cell development is pursued by some members of the PV industry. [6] By following this approach the opportunity of keeping the standard phosphorous diffused front side with conventional screen printing metallization and using high-quality *n*-type Si resulted in the evaluation of the double side contacted back-junction solar cell with rear side boron diffused emitter as recently reported by Mertens. [7]

The present work presents the double side contacted back-junction solar cell using *n*-type Czochralski grown silicon. By means of one dimensional numerical simulation the influence of bulk material properties and resistivity on the solar cell efficiency were evaluated to check the requirements on the large area *n*-type Si material. Analogous to simulations presented by

Hermle *et al.* [9] for back-junction back contact solar cells one dimensional simulation were carried out to rate the role of front side recombination on the limitation of the solar cell efficiency. The estimation of open circuit voltage ( $V_{oc}$ ) was done by experimentally determined saturation current densities ( $J_0$ ) using symmetrically processed wafers, as reported by Kluska. [8]

### 2 EXPERIMENTAL

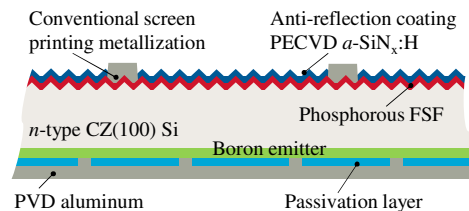


**Figure 1:** Cross section image of double side contacted *n*-type CZ Si back-junction solar cell, front side: phosphorous diffused FSF, ARC PECVD *a*-SiN<sub>x</sub>:H and screen printed metallization, rear side: boron emitter, passivation layer and PVD Al metallization

For the processing of the solar cell *n*-type Czochralski (CZ) grown Si(100) was used. The wafer had a full square area of  $A = 243.36$  cm<sup>2</sup>. The metallization was done on the front side by a standard screen printing technique and on the rear side by evaporation of aluminum. The evaporation was done using the physical vapor deposition (PVD) technique. The phosphorous diffused front surface field was passivated with 70 nm thick plasma-enhanced chemical vapor deposited (PECVD) hydrogen-rich silicon nitride (*a*-SiN<sub>x</sub>:H) with a refractive index of about  $n = 2.05$ . The boron diffused emitter on the cell rear side was coated by a dielectric layer for surface passivation. The cell structure is schematically shown in cross sectioned view in Fig. 1. For the symmetrically processed lifetime test structures the same *n*-type Si material as for the solar cells was used. The wafers had a thickness of  $W = 180$  μm. The saw-damage of the CZ wafers was removed in HNO<sub>3</sub>/HF solution followed by a KOH step. Afterwards the wafers

received a standard Radio Corporation of America (RCA) cleaning procedure. The lifetime wafers for determination of  $J_0$  of the diffused wafers received their specific passivation layer deposition after the diffusion processes and the subsequent etch treatment in diluted HF solution to etch off the doped oxide layer created during the diffusion process.

The injection dependent effective minority carrier lifetime  $\tau_{\text{eff}}$  was measured with the photo conductance decay method using a Sinton instrument WCT 120 system. [10] The determination of  $J_0$  was done in high-injection conditions from the relationship proposed by Kane and Swanson. [11]

### 3 ONE DIMENSIONAL SIMULATIONS OF LOSS MECHANISM

#### 3.1 Limitation of efficiency caused by bulk material properties

The production of high-efficiency solar cells requires the assurance of a high-quality CZ Si bulk material. When the wafer size increases this necessary condition becomes more delicate during the wafer production. Therefore the solar cell performance dependence on the wafer quality in terms of  $\tau_{\text{eff}}$  will be addressed. One dimensional numerical simulations were carried out using PC1D [12] to evaluate the impact of  $\tau_{\text{eff}}$  as a measure of Si material quality on the solar cell efficiency. The simulation was done for bulk material with a resistivity of 5  $\Omega\cdot\text{cm}$  and 15  $\Omega\cdot\text{cm}$  to address the impact of bulk conductivity (see Fig. 2). Below  $\tau_{\text{eff}} = 1$  ms a reduction of the solar cell efficiency was observed. The reduction was caused by a decrease in  $J_{\text{sc}}$ ,  $V_{\text{oc}}$  as well as  $FF$ . The material with lower doping concentration (15  $\Omega\cdot\text{cm}$ ) suffered stronger from a  $FF$ -reduction below a  $\tau_{\text{eff}}$ -value of 800  $\mu\text{s}$ .

A silicon ingot commonly consists of Si wafers in a range of resistivity. From an economic point of view the use of the complete Si ingot is desired. Therefore the question arises whether a limitation of efficiency is caused by the base doping of the CZ  $n$ -type Si material. Furthermore it is well known that each cell concept requires a specific base doping level to reach its highest cell performance, i.e. back-junction back contacted solar cells requires a medium bulk doping concentration (2-3  $\Omega\cdot\text{cm}$ ) whereas emitter-wrap through solar cells outperform at low bulk doping concentrations (>5  $\Omega\cdot\text{cm}$ ).

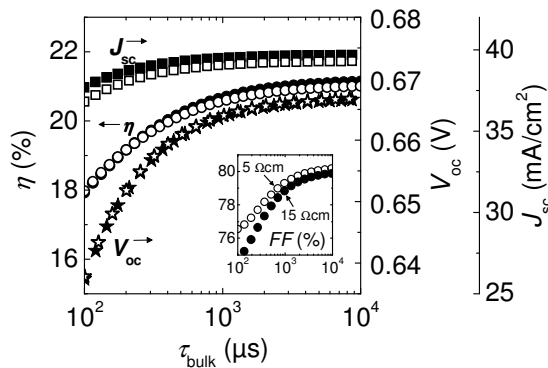


**Figure 2:** Impact of Si bulk material quality in terms of effective lifetime  $\tau_{\text{eff}}$  on solar cell parameters: efficiency  $\eta$ , fill factor  $FF$  (see inset), short-circuit current density  $J_{\text{sc}}$  and open-circuit voltage  $V_{\text{oc}}$

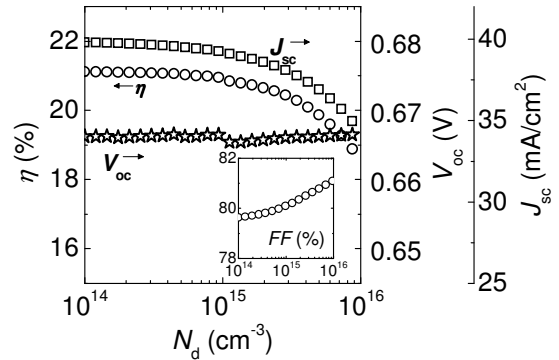


**Figure 3:** Impact of Si bulk doping  $N_d$  on solar cell parameters: efficiency  $\eta$ , fill factor  $FF$  (see inset), short-circuit current density  $J_{\text{sc}}$  and open-circuit voltage  $V_{\text{oc}}$

In Fig. 3 the impact of  $N_d$  on the solar cell parameter is shown. The simulations were done by assuming a bulk lifetime of  $\tau_{\text{eff}} = 5$  ms and excellent surface passivation properties ( $S = 10^3$   $\text{cm/s}$ ) at front and rear side to be independent of any other loss mechanism. Beyond a base doping of  $N_d > 10^{15}$   $\text{cm}^{-3}$  ( $\approx 4.6$   $\Omega\cdot\text{cm}$ ) the efficiency started to drop as caused by a reduction in  $J_{\text{sc}}$ . The increased  $J_{\text{sc}}$ -loss can be attributed to the reduction of the energy barrier provided by the FSF when  $N_d$  increased. Hence, the shielding-effect of the FSF is minimized.

#### 3.2 Front side recombination impact on solar cell efficiency

The internal quantum efficiency (IQE) describes the ratio between the  $J_{\text{sc}}$  and a photon flux  $N_{\text{ph}}$  entering the device without being reflected by the solar cell surface. [13] The IQE is given by

$$IQE(J_{\text{sc}}) = \frac{J_{\text{sc}}}{qN_{\text{ph}}(1-R)} \quad (1)$$

with  $R$  the reflection at the solar cell surface. Hermle *et al.* reported about the effect of the FSF on the IQE of back-junction back contact (BJBC) solar cells. [9] In contrast to the BJBC solar cell the base metal contact of the solar cell concept investigated in this work was not contacted to the back surface field (BSF) region on the solar cell rear side but rather to the FSF.

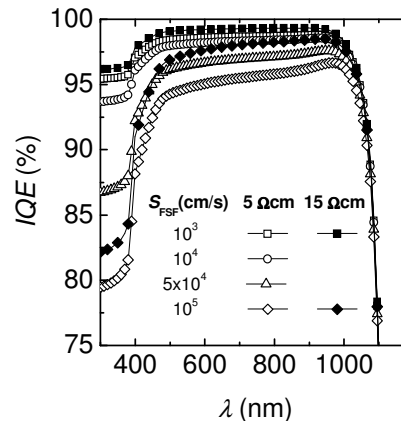


**Figure 4:** Impact of FSF recombination in terms of  $S_{\text{FSF}}$  on IQE of solar cell with resistivity  $\rho = 5$  and 15  $\Omega\cdot\text{cm}$

Therefore the question arise in which extent the described influence of FSF recombination affects the IQE of the double side contacted back-junction solar cell. To

answer this question one dimensional numerical simulation were done with PC1D. In Fig. 4 the impact of  $S_{FSF}$  on the IQE is shown. The IQE decreased with increasing  $S_{FSF}$ . The  $S_{FSF}$ -variation showed a stronger impact on the  $J_{sc}$ -loss for base material with lower resistivity. The IQE drop was caused by an increased  $S_{FSF}$  starting at about  $\lambda = 950$  nm and extending towards lower wavelengths. The dependence of the IQE on the  $S_{FSF}$  for the double side contacted back-junction solar cell was similar to the reported  $S_{FSF}$ -IQE dependence of BJBC solar cells.

#### 4 OPEN CIRCUIT VOLTAGE LIMITATIONS

##### 4.1 $V_{oc}$ -Potential calculations

The open circuit voltage limitations were calculated on the basis of experimentally determined  $J_0$ -values. The correlation between  $V_{oc}$  and  $J_0$  is:  $V_{oc} = (k \cdot T/q) \cdot \ln(J_{ph}/J_0 + 1)$  with  $J_{ph}$  the maximum current density. For the  $J_0$ -determination symmetrical processed lifetime wafers were used. The complete  $J_0$  of the double side contacted back-junction solar cell was  $J_{0,total} = 355$  fA/cm<sup>2</sup>. The bulk caused a contribution of  $J_{0,bulk} = 135$  fA/cm<sup>2</sup>. Considering the metalized fractions the  $J_0$ -contribution of the cell front side was calculated to be  $J_{0,FSF} = 191$  fA/cm<sup>2</sup> and for the cell rear side to be  $J_{0e} = 29$  fA/cm<sup>2</sup>. The  $J_0$ -contribution of the passivated and metalized fraction of the FSF was the main  $V_{oc}$ -limitation (54%). The boron emitter rear side showed the lowest contribution of 8% whereas the bulk material caused 38% of the  $V_{oc}$ -loss. An improvement of FSF passivation can be achieved on one hand by improving the  $a$ -SiN<sub>x</sub>:H front side passivation performance or on the other hand by reducing the metalized fraction on the solar cell front side. A reduction of the front side metallization can cause  $FF$ -losses due to an increase in series resistance losses which can occur when not enough conductive metal is present to assure a transport of the generated carriers. Therefore small front side grid fingers as proposed for high-efficiency solar cells on a small device area [14] cannot be implemented.

##### 4.2 Impact of rear side passivation layer on $V_{oc}$

On the basis of 25 solar cells per variation the passivation layer of the rear side boron diffused emitter was optimized. The boron emitter passivation was provided by a layer of thermal SiO<sub>2</sub> resulted in an average  $V_{oc} = 639.5$  mV. In Table I the  $J_{sc}$  and  $V_{oc}$  mean values of the rear side passivation layer variation are listed. The alternative passivation layer improved the rear surface passivation quality by  $\Delta V_{oc} = 10$  mV.

**Table I:**  $J_{sc}$  and  $V_{oc}$  mean values of 25 solar cells with different rear side passivation layer

Passivation layer	$J_{sc}$ (mA/cm <sup>2</sup> )	$V_{oc}$ (mV)
SiO <sub>2</sub> layer	38.4	639.5
Alternative layer	38.4	651.0

In Fig. 5 the 1 sun  $J$ - $V$ -characteristic of the best solar cell is shown. The solar cell provided a power output of 4.92 W and a solar cell efficiency of  $\eta = 20.2\%$  which was independently confirmed by Fraunhofer ISE CalLab. For boron emitter passivation the alternative passivation layer was used. The  $J_{sc} = 38.2$  mA/cm<sup>2</sup> showed that

shadow losses as well as the impact of the  $S_{FSF}$  has to be further optimized. A  $V_{oc}$  of 661 mV reflected the high quality of the alternative passivation layer.

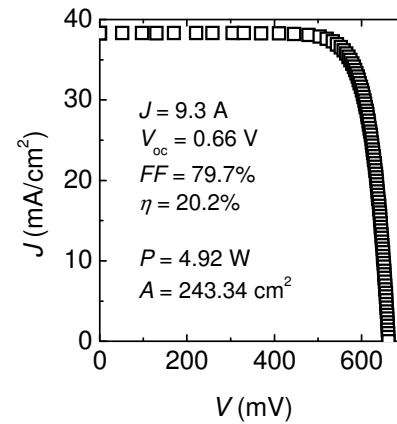


**Figure 5:**  $J$ - $V$ -characteristic of best double side contacted back-junction solar cell under 1 sun illumination

#### 5 CONCLUSION

With the double side contacted back-junction solar cell a conversion efficiency of  $\eta = 20.2\%$  is demonstrated. Hence, the feasibility of this solar cell concept is shown on large area  $n$ -type CZ Si with industrial relevant processes. For further improvement of the solar cell efficiency the front side limitations have to be reduced. In contrast to high-efficiency solar cells on a small device area for high-efficiency solar cells with a large device area the reduction of front side metal fraction can be realized in a lesser extent. It was found by one-dimensional numerical simulation that the  $J_{sc}$  is influenced by the front side recombination in same way as reported for back-junction back contact solar cells. The quality and the doping density of the bulk material play a key role in the solar cell performance.

#### 7 ACKNOWLEDGEMENTS

The authors would like to thank Dr. M. Fischer, Dr. S. Schmidt, S. Kirstein and the complete team of the Q-Cells SE Reiner-Lemoine Research Center for the experimental support. S. Bordihn would like to acknowledge Dr. D. Rychtarik for his continuous support.

This work is supported in frame of the project ALADIN (0325150) and ALBA II (0329988C) by the German federal ministry of environment, nature conservation and nuclear safety (BMU).

#### 8 REFERENCES

- [1] P.J. Cousins, 1<sup>st</sup> PV Silicon, Freiburg Germany (2011).
- [2] H. Sakata et al., 25<sup>th</sup> EUPVSEC, Valencia, Spain (2010).
- [3] F. Kiefer et al., 36<sup>th</sup> IEEE PVSC, Seattle, USA, (2011).
- [4] A. Richter et al. 23<sup>rd</sup> EUPVSEC, Valencia, Spain (2010).

- [5] S.W. Glunz *et al.*, 35<sup>th</sup> IEEE PVSC, Hawaii, USA (2010).
- [6] P. Engelhart *et al.*, 26<sup>th</sup> EUPVSEC, Hamburg, Germany (2011).
- [7] V. Mertens *et al.*, nPV Workshop, Konstanz, Germany (2011).
- [8] S. Kluska *et al.*, 23<sup>rd</sup> EUPVSEC, Valencia, Spain (2008).
- [9] M. Hermle *et al.*, J. Appl. Phys. 103, 054507 (2008).
- [10] R. A. Sinton and A. Cuevas, Appl. Phys. Lett. 69, 2510 (1996).
- [11] D.E. Kane, R.M. Swanson, 18<sup>th</sup> IEEE PVSC, Las Vegas, USA (1985).
- [12] P.A. Basore, D.T. Rover, and A.W. Smith, 20<sup>th</sup> IEEE PVSC, (1988).
- [13] H. Mäckel, and A. Cuevas, J. Appl. Phys. 98, 083708 (2005).
- [14] J. Benick *et al.*, Appl. Phys. Lett. 92 253504/1 (2008).